Journal of Experimental Psychology: Applied
2002, Vol. 8, No. 2, 99–117

1076-898X/02/$5.00 DOI: 10.1037//1076-898X.8.2.99

Investigating Spatial Vision and Dynamic Attentional Selection Using a Gaze-Contingent Multiresolutional Display

Lester C. Loschky and George W. McConkie
University of Illinois at Urbana–Champaign

This study examined spatial vision and attentional selection using a gaze-contingent multiresolutional display, with a dynamic, gaze-centered, high-resolution *window* and lower resolution periphery. Visual search times and eye movements from 15 participants in a 3 × 3 design (Window Radius × Peripheral Resolution) suggest that contrast sensitivity as a function of retinal eccentricity affects attentional selection and visual processing. Smaller windows led to longer search times and shorter saccades; lower peripheral resolution also shortened saccades (all *p*s < .05) as a result of avoiding fixating degraded areas. Fixation durations, although longer for smaller windows ($p < .05$), were unaffected by whether the next saccade went within or outside the window. These results are explained through (a) competition among potential saccade targets where above-threshold filtering reduces an object's relative salience and (b) generally disrupted visual processing.

GAZE-CONTINGENT MULTIRESOLUTIONAL DISPLAYS

Over the past 20 years, there has been a push to develop computer displays that have a large field of view, high resolution, and fast frame rates in order to enhance viewers' perceptual experience. Such displays are needed for a number of single-user display applications such as simulators (for flight, driving, or medicine), virtual reality, video telephony, telemedicine, teleoperation, and remote piloting. However, such extreme demands on a display frequently exceed the available transmission bandwidth or processing limitations. A solution proposed by electrical engineers takes advantage of a fundamental characteristic of the human visual system: the reduction of visual resolution with retinal eccentricity. If, at any given moment, high resolution is put only at the center of gaze and reduced elsewhere, one can greatly reduce bandwidth and computation requirements. For example, an image can be progressively transmitted over a limited bandwidth channel, with high-resolution information first sent to the point of gaze (e.g., Wang & Bovik, 2001). We refer to such a display, which dynamically modifies resolution across the image in real time in response to an observer's shifts of gaze, as a *gaze-contingent multiresolutional display*, or GCMRD (for review, see Reingold, Loschky, McConkie, & Stampe, in press).

Theoretically, an appropriately designed GCMRD would produce the experience of looking at a normal, high-resolution image while using only a fraction of the normally required resources. The attempt to create such a display raises psychological issues, a number of which are discussed by Reingold et al. (in press). The current study investigates the effects of the size of the high-resolution region and the degree of image filtering in the peripheral region on observers' search-task performance and eye movements when examining complex monochrome photographic images. Although such research should be useful in developing GCMRDs, it should also be valuable for theories of perception because it shows the nature of the stimulus requirements for normal viewing of complex stimuli and the operation of the human visual system (HVS) when stimuli are inadequate. Of particular interest is how above-threshold filtering of visual information affects attentional selection as indicated by an observer's eye behavior.

IMAGE FILTERING, VARIABLE RESOLUTION OF THE HVS, AND ATTENTIONAL SELECTION

If we start with a constant-resolution image and plan to transmit its high-resolution information only to the center of vision, we must begin by filtering out the high-resolution information everywhere else. We call this process *multiresolutional image filtering* (see Reingold et al., in press, for a summary of methods that have been used with GCMRDs). Most filtering methods involve iteratively low-pass filtering and subsampling the image (Moulin, 2000). Low-pass filtering of higher spatial frequencies (i.e., removing fine detail) is accomplished by reducing the contrast of those frequencies. The process of low-pass filtering can be related to visual perception, because if the contrast of a given spatial

Lester C. Loschky, Department of Psychology, University of Illinois at Urbana–Champaign; George W. McConkie, Department of Educational Psychology, University of Illinois at Urbana–Champaign.

Parts of this study were previously presented in talks at the Annual Federated Laboratory Symposium on Advanced Displays and Interactive Displays (1997, 1999) and the Eye Tracking Research & Applications Symposium (2000), with brief versions of the talks published in the proceedings of those symposia. This work was supported by funds from the Beckman Institute and from the University of Illinois Research Board, and by U.S. Army Research Laboratory under the Federated Laboratory Program, Cooperative Agreement DAAL01-96-2-0003. The National Institute of Mental Health provided funds for purchasing eye-tracking equipment, and the National Science Foundation provided other essential equipment under Grant CDA 96-24396. We thank Gary Wolverton, who developed the system and wrote the software that made this research possible, and also Ed Niu for providing the wavelet decomposition and reconstruction algorithm. Dave Irwin, Art Kramer, Gordon Logan, and Greg Zelinsky all provided helpful comments on earlier versions of this article, and George Russell carefully proofread the final manuscript.

Correspondence concerning this article should be addressed to Lester C. Loschky, who is now at the Human Perception & Performance Group, Beckman Institute for Advanced Science and Technology, 405 North Mathews, Urbana, Illinois 61801. E-mail: loschky@uiuc.edu

frequency is too low, we do not perceive it. The range of spatial frequencies that are visible, as measured by our sensitivity to contrast at each frequency, is described by a contrast sensitivity function, that is, "a graph depicting a person's ability to see targets of various spatial frequency; on the x-axis is the spatial frequency of the test target; on the y-axis is . . . the minimum contrast needed to see the test target" (Sekuler & Blake, 2002, p. 614). More important, contrast sensitivity to different spatial frequencies also varies as a function of retinal eccentricity (Anderson, Mullen, & Hess, 1991; Banks, Sekuler, & Anderson, 1991; Cannon, 1985; Peli, Yang, & Goldstein, 1991; Pointer & Hess, 1989; Robson & Graham, 1981). The most common psychophysical measures of contrast sensitivity are the ability to discriminate a grating from an even gray patch and the ability to discriminate the orientation of a grating. Figure 1 (Yang, Coia, & Miller, 2001), which is based on the orientation discrimination measure, shows that contrast thresholds as a function of retinal eccentricity increase much more quickly for higher spatial frequencies than for lower frequencies, that is, perception of fine detail rapidly diminishes with distance from the center of vision.

The above findings suggest that the perceptibility of filtering in image regions should vary with their spatial frequency bandwidth and retinal eccentricity (Geisler & Perry, 1998; Peli & Geri, 2001; Yang et al., 2001). If low-pass filtering of an image removes, at various eccentricities, only subthreshold spatial frequencies, it should produce a normal perceptual experience. Conversely, if above-threshold spatial frequencies are removed at any eccentricity, the existence of filtering may be perceived. This assumption has recently been supported by studies using tachistoscopically presented multiresolutional versions of photographs in which participants performed either image discrimination (Peli & Geri, 2001) or image-quality-rating tasks (Yang et al., 2001). However, during dynamic image viewing, what effect does such image filtering have on the interface of perception and action, attentional selection?

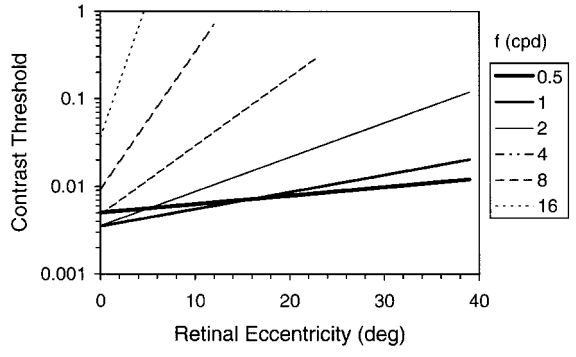

Figure 1. Contrast thresholds as a function of spatial frequency (f) and retinal eccentricity. Stimuli were statically presented and ranged in spatial frequency from 0.5 to 16 cycles per degree (cpd). deg = degrees visual angle. From "Subjective Evaluation of Retinal-Dependent Image Degradations," by J. Yang, T. Coia, and M. Miller, 2001, *Proceedings of the IS&T's 2001 PICS Conference*, p. 143. Copyright 2001 by The Society for Imaging Science and Technology. Reprinted with permission.

Possible Effects of Filtering on Attentional Selection

Stimulus Characteristics, Saliency, and Attentional Selection

A key question for researchers in scene perception is: What determines where a person will attend in a display? We assume that there are *preattentive* processes that select a location or region for attention. Such processes appear to perform basic visual analyses before object recognition, and their output is often described in terms of fundamental *features*, such as orientation, color, motion, size, and so forth (Wolfe, 1994). Whether a stimulus characteristic can be considered a preattentive feature is usually determined by the ease with which it can be used to find a target in a search task or to segregate a texture display (Julesz, 1981; Treisman & Gelade, 1980; Wolfe, 1994). Thus, preattentively available features make targets *pop out* in visual search and texture displays (e.g., a red object among green objects) regardless of the number of items in the display. Studies have shown the pop-out phenomenon based on spatial frequencies, and therefore spatial frequency information appears to be preattentively available as well (Moraglia, 1989; Sagi, 1988).

Most theories of attentional selection suggest that preattentive features are contained in separate topographical maps of the visual array (Itti & Koch, 2000, 2001; Koch & Ullman, 1985; Treisman & Gelade, 1980; Wolfe, 1994). There is evidence that spatial-frequency feature maps exist in visual cortex, as shown by neurophysiological studies of cats and macaques (Issa, Trepel, & Stryker, 2000; Silverman, Grosof, De Valois, & Elfar, 1989). It is assumed that, within each feature map, the selection of a target for attention is determined by a competition, in which the most distinctive, or *salient* feature in a map is the winner. If the viewer has not been cued to a particular feature, then the location in visual space having the highest activation across all activated feature maps would be most salient, and chosen as the target for attention (Itti & Koch, 2000, 2001; Koch & Ullman, 1985; Wolfe, 1994).

Observing where a viewer's eyes go in picture viewing is another way of measuring attentional selection. This is based on the well-tested assumption that attention inevitably precedes the eyes to a location (Deubel & Schneider, 1996; Hoffman & Subramaniam, 1995; Irwin, Colcombe, Kramer, & Hahn, 2000; Irwin & Gordon, 1998; Kowler, Anderson, Dosher, & Blaser, 1995). Furthermore, single-cell recordings in macaques have shown that brain areas associated with eye movement targeting and attentional allocation (e.g., the frontal eye fields, the posterior parietal cortex, and the superior colliculus) appear to have saliency maps of the visual field, with locations having more salient features showing greater activation (Colby & Goldberg, 1999; Gottlieb, Kusunoki, & Goldberg, 1998; Kustov & Robinson, 1996; Schall & Bichot, 1998; Schall, Hanes, Thompson, & King, 1995). If these findings scale up to normal picture viewing, then we should be able to determine the relative salience of various features by measuring the probability of the eyes moving to different locations, assuming that the most salient items would be preferentially targeted. Thus, several recent studies have asked viewers to visually explore photographic images (e.g., in preparation for a memory test), and the resultant fixation patterns have been analyzed as a function of such stimulus characteristics as contrast, spatial frequency, and edges (Krieger, Rentschler, Hauske, Schill, & Zetzsche, 2000;

Mannan, Ruddock, & Wooding, 1997; Reinagel & Zador, 1999). Mannan et al. (1997) found that spatially localized measures of high-spatial frequency content, local luminance contrast, and edge density only weakly differentiated randomly selected locations from actual eye fixation locations. Reinagel and Zador (1999) found somewhat higher contrast around viewers' fixation points compared with randomly selected areas from those images, with the heightened contrast diminishing within 4° of fixation. Similarly, Krieger et al. (2000) found that fixated regions had greater luminance variability (i.e., contrast). They also observed a slightly greater tendency to fixate higher spatial frequency regions than predicted by chance. Together, these results suggest that higher contrast and higher spatial frequencies exert a weak but consistent effect on where viewers fixate during picture viewing.

Spatial Image Filtering and Visual Saliency

Consideration of the above findings leads us to ask: What effect does multiresolutional image filtering have on visual saliency, and thus attentional selection, as measured by eye movements or visual search in normal image viewing? Unfortunately, few studies have addressed these issues. Mannan, Ruddock, and Wooding (1995) had viewers look at high-pass, low-pass, and unfiltered versions of photographs and measured the effects on their eye movements. They found that low-pass filtered images led to longer fixation durations than did either high-pass or unfiltered images, but that both high-pass and low-pass filtered images produced shorter eye movements, that is, *saccades*, than unfiltered images did. Thus, the results of Mannan et al. (1995) suggest that image filtering affects salience as measured by eye movements, but their results are difficult to interpret in terms of our particular concerns. First, the saccade length measure, which should be most closely tied to attentional selection, showed no clear difference between high- and low-pass filtering. Second, their images were uniformly filtered across the entire image; therefore, we do not know whether it was the filtering of the image at the fovea, in the periphery, or both that affected saccade lengths and fixation durations.

A study by Shioiri and Ikeda (1989) investigated the effect of degrading information outside of a high-resolution gaze-contingent *window* on eye movements. They found that participants' median saccade lengths were reduced in conditions of higher peripheral degradation. Likewise, median saccade lengths were reduced as the size of the gaze-contingent undegraded region became smaller. Nevertheless, for the purpose of our discussion, it is unclear how these results can help explain the relationship between spatial filtering and salience. This is because the method of image degradation used in their study was to add random spatial noise to their base images, which is unlikely to have reduced their higher spatial frequency content, though this method might possibly have masked some of the higher spatial frequencies. Thus, although their use of a GCMRD and their analysis of eye movement data are relevant to the questions we are raising, the fact that their method of image degradation only bears indirectly on the issue of image-spatial-frequency content renders their results inconclusive for our purposes.

Summary

Recent work attempting to reduce the bandwidth and computing resources required to produce large, high-resolution displays has indicated the potential of GCMRDs. However, to make useful GCMRDs requires an understanding of the effects of eliminating selected spatial frequencies in the visual periphery on perception and attention. Although removing higher spatial frequencies in visual regions where they are below the contrast threshold should have little or no effect, the effect of removing above-threshold frequencies needs investigation. There is evidence that filtering images, either low- or high-pass, affects the lengths of observers' saccades (Mannan et al., 1995). Because attention precedes saccades, we assume that these changes in eye behavior reflect preattentive processes that lead to oculomotor choices (Deubel, 1991; Motter & Belky, 1998; Thompson, Bichot, & Schall, 2001; Williams & Reingold, 2001). Specifically, spatial frequency bands may be a feature of image regions that affects their salience in competing for attention and saccades.

OVERVIEW OF THE STUDY

In our experiment, we measured participants' eye movements as they performed a search task and a memory task during free viewing of a set of complex images. These images were presented in a bi-resolutional GCMRD, having high resolution at the center of gaze on each fixation and wavelet-based low-pass filtering elsewhere. The radius of the high-resolution area (the window) and the degree of filtering over the rest of the image were varied factorially across images for each participant in a counterbalanced design. We then examined the effects of window radius and filtering level on search times and eye movement measures. On the basis of previous research, we predicted that reducing the window radius or increasing the level of peripheral filtering would increase search time, shorten saccades, and increase fixation durations during the perception of complex photographic images. Our first task was therefore to identify those levels of peripheral spatial filtering and window radius (i.e., retinal eccentricity at which filtering begins) that were indistinguishable from the full high-resolution control. Then, using eye movements as our most detailed measure of attentional selection, we identified functions relating these measures to the elimination of higher spatial frequencies at different retinal eccentricities. Finally, we tested alternative hypotheses regarding the effect of spatial frequency filtering at varying retinal eccentricities on where and when the eyes move during picture viewing.

EXPERIMENT

Method

Participants

There were 15 paid adult participants (7 women), from the University of Illinois at Urbana–Champaign, all with normal uncorrected vision.

Stimuli

The stimuli consisted of 2 sets of 15 monochrome, 8-bit resolution photographs shown on a computer monitor (described below). The first set of 15 original images was used to create a second set of 15 modified versions used as foils in same–different recognition tests. The subject matter of the images was extremely varied (from street scenes to building interiors), and all contained a large amount of visual detail (see Figure 2 for

Figure 2. Example images used in the study with varying window radii and peripheral filtering resolution levels. Panel A = smallest window (radius = 1.6°) with lowest filtering resolution (Level 1); Panel B = medium window (radius = 2.9°) with medium filtering resolution (Level 4); Panel C = largest window (radius = 4.1°) with higher filtering resolution (Level 7); Panel D = control condition (constant highest level resolution). Obtained from the Corel Image Database.

one image in four resolution conditions). Images measured 768 pixels × 512 lines and subtended 18° × 12° visual angle.

There are many ways of creating multiresolutional images (see Reingold et al., 2001, for a review and comparison of methods), but the conceptually simplest approach is to make what we call a *biresolutional image* with a high-resolution region (the window) at some specified location surrounded by a lower resolution peripheral region. In the current study, we used biresolutional images in which peripheral image resolution was reduced through image filtering by using the *discrete wavelet transform.* The discrete wavelet transform is an attractive form of multiresolutional image representation for purposes of image compression because it is complete yet sparse, whereas other methods such as Gaussian and Laplacian Pyramids are *overcomplete;* that is, the multiresolutional representation is roughly 33% larger than the original (Moulin, 2000). Furthermore, the hierarchical structure of wavelet image representations allows them to be truncated in specific image regions where only lower resolution is needed, as in progressive transmission applications (Wang & Bovik, 2001).

In the current study, we first transformed the images by carrying out a four-stage wavelet decomposition of each image into four bands of increasingly higher spatial frequencies, each an octave apart, using the 9/7 symmetric biorthogonal wavelet basis function described by Antonini, Barlaud, Mathieu, and Daubechies (1992, p. 208, filter tap values given on p. 209). This transformation resulted in a total of 13 subbands, each having an associated set of coefficients. Images were then reconstructed while we eliminated varying numbers of higher frequency subbands. Using all 13 subbands recreated the original image; including only some of them resulted in a low-pass filtered image (Figure 2; see Niu, 1995, for a detailed description of the image filtering). Because of the particular characteristics of wavelet subband coding, within a 13 subband set, we were only interested in images reconstructed with the first 1, 4, 7, 10, or 13 subbands. Images reconstructed with any other number of subbands would lack details in specific orientations (horizontal, vertical, or diagonal; for a wavelets tutorial, see Moulin, 2000). For reasons explained below, we did not use the filtering condition that included the first 10 subbands.

We then used the discrete wavelet transform to create biresolutional images; that is, we included all of the subbands in the high-resolution window, and only the specified subbands with their associated lower spatial frequencies outside that region. Furthermore, the edge was smoothed because of the rounding of coefficients at the boundary between the higher and lower resolution areas. For each Window Radius × Peripheral Filtering Level combination, we prepared a set of 330 versions of each picture. All versions were created by superimposing a 22 × 15 imaginary

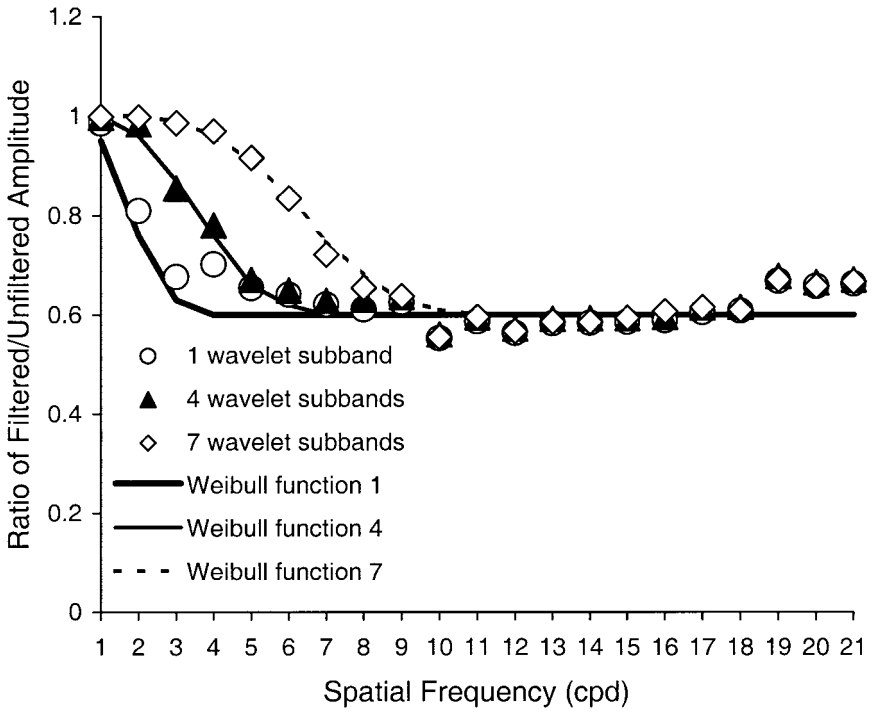

Figure 3. Empirically derived spatial frequency bandpass characteristics of the three peripheral filtering conditions in the study. Filters included either 1, 4, or 7 wavelet subbands in reconstructing the peripheral image areas. The ordinate shows the ratio of mean energy level (amplitude) across the sample filtered images relative to their unfiltered versions. The abscissa shows spatial frequency in cycles per degree (cpd). Symbols represent empirical data values for each filter and solid and hatched lines represent the modified Weibull functions that best fit the data for each filter.

grid over each 18° × 12° picture with roughly 0.82° between grid points. At each of the 330 points in the grid, an image version was created with its center of high resolution at that grid point. In this way, wherever viewers looked, there was an image version whose center of high resolution was within 0.41° (horizontally or vertically) of their center of gaze.

To determine empirically the spatial frequency characteristics of the different levels of filtering used, we carried out a Fourier analysis on a sample of 10 images used in this and other studies in our lab. The analysis included the same images in each of the filtering conditions used in this experiment, including the 13 subband (i.e., no-filtering) control condition. Then, across the 10 images, we calculated the average amplitude for each spatial frequency from 1–21 cycles per degree (cpd). Next, we calculated the ratio of the average amplitude (A) for each spatial frequency (f) for each filtering condition to the corresponding average for the no-filtering control. Thus, a ratio of unity for a given spatial frequency in a given filtering condition indicates that no filtering occurred at that frequency, whereas a ratio less than one indicates a loss of energy at that frequency. Finally, an equation was fit to the data in each filtering condition, which were well described by a modified Weibull function with two parameters, c1 and c2:

$$A(f) = 1 - 0.4 \times \{1 - \exp[-(f/c1)^{c2}]\}.$$

The results of the analysis are shown in Figure 3.[1] The graph shows that, indeed, as fewer wavelet subbands are included in the reconstructed images, higher spatial frequencies become more attenuated, leaving greater energy only at the lower frequencies. Even the highest resolution-filtering condition shown in Figure 3, which includes the first 7 subbands, shows attenuation of spatial frequencies in the range of roughly 5–21 cpd. Figure 1 indicates that viewers are quite sensitive to many of the frequencies in this range in both peripheral and parafoveal vision; that is, the filtering levels shown in Figure 3 remove many spatial frequencies that are above-threshold in the parafovea or visual periphery.

Design

A 3 × 3 randomized blocks, within-subjects, factorial design was used, with three levels of peripheral filtering resolution (using the first 1, 4, or 7 wavelet subbands) and three window radii (1.6°, 2.9°, and 4.1°). In addition, a control condition was included in which the entire image was shown in high resolution (i.e., using the complete set of 13 wavelet subbands). The three levels of peripheral filtering were chosen on the basis of results from a previous study in which biresolutional images were flashed for 150 ms and participants were asked to indicate whether they detected peripheral image degradation (Loschky & McConkie, 2000). That study showed that although all three filtering levels produced detectable image degradation with window radii as large as 4°, there was nevertheless a wide range of detectability as a function of filtering level. The filtering level including the first 10 subbands was not used because it was undetectable with any of the window sizes we intended to use. The window radii used in the study were chosen to provide a reasonable range of retinal eccentricities from which to begin extrafoveal filtering. The smallest radius, 1.6°, is larger than standard estimates of the foveola, which is roughly 0.5–1.0° in diameter, that is, 0.25–0.5° radius (Boff & Lincoln, 1988). Thus, an error in window placement of greater than 1° would be required to bring the closest filtered region within the foveola. The largest radius, 4.1°, is near the limit—

[1] We thank Jian Yang for help in doing this analysis.

around 5°—of the "useful field of view" as estimated by Shioiri and Ikeda (1989), and results in a high-resolution window containing roughly 25% of the full screen area. By leaving at least 75% of the image area within the filtered periphery, we ensured that we could find the effects of a filtered periphery on perception and eye movements; using much larger window radii would have left little image area outside the high-resolution window to show such effects. The order of experimental conditions was completely counterbalanced across participants.

Apparatus

In the experiment, participants performed visual search and picture-recognition memory tasks. In carrying out these tasks, participants viewed the aforementioned complex, photographic images with both eyes using a gaze-contingent, biresolutional display. There are important technical issues in using GCMRDs regarding the method of image updating and the speed with which it occurs (Reingold et al., in press). The area of high resolution in the image moves with the eye, and thus creates a type of image motion; that is, the level of detail at different areas of the image changes in real time. In fact, there has been very little research investigating the perception and performance effects of stimulus motion produced by the image updating process in GCMRDs. Nevertheless, several steps were taken to eliminate the perception of such image motion. To begin with, images were updated only at the ends of saccades, during saccadic suppression (Burr, Morrone, & Ross, 1994; Shioiri & Cavanagh, 1989). Such updating, however, requires that the center of high resolution be changed to the new point of gaze very rapidly. Otherwise, if the change in the image occurs long after saccadic suppression has dissipated, image motion may be perceived. Therefore, the current study used a system designed to minimize image-updating delay. First, movements of each participant's right eye were recorded with a Dual Purkinje Generation III eyetracker, with the output sampled at 1,000 Hz (1 sample per ms), thus providing high temporal resolution in identifying the ends of saccades. Second, to avoid online image generation time, all 330 versions of each image were prestored in a ViewGraphics ViewStore (ViewGraphics Incorporated) 1 GB image memory and display controller. Third, the image version corresponding to the imaginary grid point closest to the viewer's fixation point was sent to the display monitor within 5 ms of the end of each saccade based on the results of a separate study (Loschky & McConkie, 2000; McConkie & Loschky, 2002) showing that this deadline eliminated perception of such image motion. Fourth, the monitor was a Conrac Mars 9320 using a refresh rate of 60 Hz, and image changes could be made at any point during the refresh cycle, thus reducing the delay between the request for an image version and its appearance on the screen. In sum, the methods used to update the position of the GCMRD in the current experiment allow greater confidence that the effects observed are the result of the spatial frequency characteristics of the image rather than the result of perceived image motion.

Procedure

Before beginning the experiment, participants completed two example search tasks and four example memory tests of the type used in the experiment and received feedback on their accuracy. They were also shown an example biresolutional image and were told that in the experiment, the high-resolution window would move wherever their eyes moved. Any questions about the general procedures were then answered. Following this orientation, participants were seated at the eyetracker for calibration, which involved their looking sequentially at each of nine points in a 3×3 grid on the computer monitor twice and pressing a button while fixating each point. The two eye position samples obtained from each point were compared, and if they differed by 0.26° or more, that location was resampled, with the process continuing until all nine points met the difference criterion. Participants were recalibrated after every 20 trials.

The search task portion of the experiment consisted of 30 trials (18 experimental, 12 control) per participant. Each of the 15 original images was used for 2 different search trials, each trial having a different search target. Each search block consisted of the presentation of five images, three with peripheral filtering and two without (control condition). A trial began when a written search-target prompt appeared on the screen (e.g., "Find the grocery bag"). When ready, the participant pressed a button and a fixation point appeared at one of nine locations on the screen, divided by a 3×3 grid. The fixation point was never less than 5° from where the target would be when the picture appeared, thus ensuring that the target would never start out within the high-resolution area, even in the largest window condition. The participant pressed the button again and 750 ms later, the search picture appeared on the screen. The participant pressed the button as soon as the target was located, and thus ended the trial.

The memory task portion of the experiment consisted of 30 trials (18 experimental, 12 control) per participant. The learning phase of the memory task followed the search tasks. Participants were shown each original image again for 20 s in preparation for a same–different recognition test. Each trial began with a fixation point at the center of the screen, and, when ready, the participant pushed a button to begin the trial. The picture appeared 750 ms later and remained on the screen for 20 s. Each learning phase block consisted of the presentation of five original images, three with peripheral filtering and two without (control condition). The test phase then followed, in which the participant viewed the same five images (three originals, two modified versions) for 20 s each, followed by a recognition test prompt asking whether the picture had been exactly the same or in any way different from one seen before (with the participant responding by pressing one of two buttons). The modified versions differed from the originals either by a change in detail (adding, deleting, moving, or switching of objects) or by being horizontally flipped (i.e., mirror reversed). Only control trial images were in fact modified. To encourage detailed viewing of all pictures, participants were not given feedback regarding their recognition accuracy during the experiment.

Results and Discussion

Overview

The results of the study, and their discussion, are divided into three sections concerning (a) participants' search times, (b) their accuracy in the memory task, and (c) their eye movements while carrying out the search and memory tasks. The eye movement analysis section is further divided into three main subsections. The first eye movement subsection analyzes the effects of peripheral filtering on global eye movement parameters, such as total number of fixations per trial, mean fixation durations, and mean saccade lengths. This section also examines correlations among these eye movement measures and search times in an effort to explain their interrelations. The second eye movement subsection asks how peripheral filtering affects where the eyes are sent. This section examines three alternative hypotheses for explaining the effects of peripheral filtering on how far the eyes travel with each saccade. The third eye movement subsection asks how peripheral filtering affects when the eyes leave their current location. This section builds on the previous one by examining the relationship between the duration of the current fixation and the saccade targeting process, as indicated by where the following eye movement is sent.

Search Times

To normalize the positively skewed search time distribution, we used a log transformation and excluded one extremely long, out-

lying search time. Then, we analyzed the data with a two-way within-subjects analysis of variance (ANOVA; Window Radius × Peripheral Filtering Level, see Table 1). We excluded one participant's data from this analysis because of missing data in one cell of the design. The alpha level was set at .05 for all statistical tests. As expected, smaller window radii produced longer search times. Contrary to expectations, however, neither peripheral filtering level nor its interaction with window radius significantly affected the time taken to search for objects. The lack of a main effect for peripheral filtering level may have been caused by either a lack of power (observed power at $p = .05$ was only 0.20) or the range of filtering levels used (1, 4, and 7), all of which were peripherally detectable according to a previous study (Loschky & McConkie, 2000). Clearly, adding an undetectable level of filtering to the range of filtering levels used would probably produce a significant filtering main effect.

We also carried out planned comparisons of the control condition against all combinations of window radius and peripheral filtering level. The results of this analysis are shown in Figure 4, with 95% confidence intervals for the difference between each experimental condition and the full high-resolution control. However, for clarity of presentation, Figure 4 shows only the confidence intervals for filtering conditions that differed significantly from the control condition. These intervals are for the two higher levels of filtering, 1 and 4, and they differed from the control condition only at the smallest window radius, 1.6°. Again, these results can be partly explained in terms of a lack of power, as indicated by the large error bars in Figure 4; however, inspection of this figure also indicates that search times in the 4.1° radius window condition were very close to those in the control condition, particularly in Filtering Level 7.

Visual search is a widely used measure of attentional selection. As anticipated, the process of visual search was adversely affected by the levels of peripheral filtering used in our study; as the radius of the high-resolution window decreased, bringing the region of lower resolution closer to the fovea, search times increased. There are several possible explanations for this occurrence. First, the filtered peripheral information might disturb processing, increasing fixation durations. Second, if filtering reduces the salience of peripheral objects, the eyes may go to closer objects located in the high-resolution window, thus reducing saccade length. Third, peripheral filtering may make it necessary for the eyes to be closer to the target in order to detect it, suggesting that, on average, more fixations would be needed to detect the target. These alternatives are not exclusive—more than one of the effects could be occurring—and need to be explored in the eye movement data analysis.

Table 1
Within-Subjects Analysis of Variance for Log_{10} Search Times as a Function of Window Radius and Peripheral Filtering Level

Source	*df*	*F*	Cohen's *f*
Blocks (B)	1	823.64*	—
Error (B)	13	(0.14)	
Window Radius × B	2	5.45*	0.27
Error (Window Radius × B)	26	(0.05)	
Filter × B	2	0.97	0.00
Error (Filter × B)	26	(0.08)	
Window Radius × Filter × B	4	0.23	0.00
Error (Window Radius × Filter × B)	52	(0.09)	

Note. Values enclosed in parentheses represent mean square errors. Cohen's *f* (dash; Kirk, 1995, p. 460) not calculated as this is a nuisance variable.
* $p < .01$.

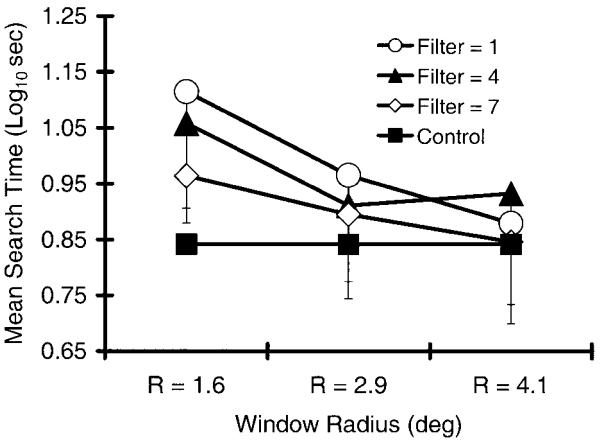

Figure 4. Mean $\log_{10}$ search times in seconds (sec) as a function of window radius, in degrees visual angle and filtering resolution level. R = the window radius, in degrees of visual angle (deg); Filter = filtering resolution level measured as number of wavelet subbands used in the wavelet reconstruction out of a total of 13, with fewer subbands resulting in lower resolution; Control = constant highest resolution image. Error bars represent 95% confidence intervals (two-tailed) for each condition versus the full high-resolution control condition.

Conversely, as the radius of a high-resolution window increased, search times decreased to the point that with a window radius of 4.1°, search times were no different from the constant high-resolution control condition. Thus, it is possible to achieve normal search performance with peripheral filtering that is at least nominally detectable. Nevertheless, we did not find the expected main effect for level of filtering resolution, or its interaction with window radius, possibly because of the limited number of observations for each participant in each condition. Thus, to make a more detailed and robust analysis of the effects of above-threshold peripheral image filtering on attentional selection, we can examine eye movement data from this task. In addition, we also collected eye movement data in the recognition-memory task, in which the time spent looking at each picture was generally longer, thus providing us with a larger and more stable pool of data.

Memory Task Performance

The function of the recognition-memory task was simply to encourage detailed viewing of the images for the full 20 s of each memory task trial. Participants were relatively sensitive, with an average recognition accuracy of 76% (72% hits and 19% false alarms). They were also slightly biased toward responding that pictures had changed; the average proportion of "different" responses across changed and unchanged trials was 54%, whereas the actual proportion of changed trials was 40%. In sum, it appears that the participants were thoroughly engaged in the memory task as intended.

Eye Movements

Analysis of Global Eye Movement Parameters

To reduce skewing in the data by extreme outliers, we excluded the 1st and 99th percentiles of the fixation duration and saccade length distributions from the analyses. The resulting data set contained a total of 39,485 saccade-and-fixation pairs. Fixations ranged in duration from 69–899 ms ($M = 280$ ms, $SD = 130$ ms). Saccades ranged in length from 0.02° to 11.72° ($M = 2.25°$, $SD = 1.95°$). The alpha level was set at .05 for all statistical tests.

Mean total fixations per trial. This analysis was done only for the search task data because it is relevant to explaining the search time results, and because the number of fixations in the memory task was constrained by a time limit. We performed a two-way within-subjects ANOVA on the mean fixations per trial in the search task. This analysis showed no significant effect of window radius, peripheral filtering level, or the interaction of the two (radius main effect), $F(1.42, 18.52$ [box epsilon]$) = 3.22$, $p > .05$, Cohen's $f = 0.18$; filtering main effect, $F(2, 26) < 1$; interaction, $F(4, 52) < 1$. Planned comparisons of all Window Radius × Peripheral Filtering Level conditions versus the full high-resolution control condition likewise failed to show any significant differences.

Mean fixation durations. Because the time limit in the memory condition placed almost no constraint on the durations of fixations, we carried out a three-way within-subjects ANOVA for task (search vs. memory), window radius, and peripheral filtering level (see Table 2). This analysis showed no significant main effect for task (search: $M = 295$ ms, $SE = 10$ ms; memory: $M = 287$ ms, $SE = 8$ ms), or interactions involving task. Thus, for all further analyses of fixation duration, we have pooled the data across tasks.

As Table 2 indicates, there was a significant main effect and a large effect size (Cohen's $f = 0.46$) for window radius on fixation durations, but there was neither a significant main effect for peripheral filtering level nor any significant interactions involving it. We also performed planned comparisons of the control condition versus all combinations of window radius and peripheral filtering level. The results are shown in Figure 5, with 95% confidence intervals for the difference of each Radius × Filtering Condition versus the control condition. Fixation durations in the small (1.6°) and medium (2.9°) window radius conditions were significantly longer than those in the control condition, but fixation durations in the largest window radius condition (4.1°) were not. This pattern of results is in agreement, then, with that for search time.

Fixation durations are often assumed to reflect foveal processing (Findlay & Walker, 1999; van Diepen, Ruelens, & d'Ydewalle, 1999). It is interesting, then, that the mean fixation durations differed across the window radius conditions when none of the conditions should have involved filtering in the fovea itself. Having a filtered stimulus within 2.9° of the center of vision still appears to affect processing, but by 4.1° eccentricity, the filtering appears to have little or no effect on fixation durations. If the processing difficulty indicated by the increased fixation durations was due to inadequate visual information in the filtered peripheral region, then we would expect that more severe filtering (removing more high-frequency information) would cause greater difficulty, thereby further increasing fixation durations. However, within the range of filtering levels tested, fixation durations varied little with the level of filtering. Thus, the current results suggest that the presence of detectable peripheral filtering, rather than the level of detectability of that filtering, affects the durations of fixations.

Mean saccade lengths. Table 3 shows a three-way within-subjects ANOVA on mean saccade lengths, as a function of task, window radius, and peripheral filtering level. As with mean fixation durations, there was no significant main effect for task nor were there any significant interactions involving task. Therefore, in all further analyses of saccade lengths, the data from both tasks (search and memory) have been pooled.

Table 2
Within-Subjects Analysis of Variance for Fixation Durations as a Function of Task, Window Radius, and Peripheral Filtering Level

Source	*df*	*F*	Cohen's *f*
Blocks (B)	1	1177.96*	—
Error (B)	14	(19413.73)	
Task × B	1	2.38	0.07
Error (Task × B)	14	(2204.29)	
Window Radius × B	2	30.02*	0.46
Error (Window Radius × B)	28	(719.92)	
Filter × B	2	0.36	0.00
Error (Filter × B)	28	(1212.36)	
Task × Window Radius × B	2	0.30	0.00
Error (Task × Window Radius × B)	28	(479.48)	
Task × Filter × B	2	0.82	0.00
Error (Task × Filter × B)	28	(522.79)	
Window Radius × Filter × B	4	1.02	0.02
Error (Window Radius × Filter × B)	56	(881.67)	
Task × Window Radius × Filter × B	4	1.82	0.11
Error (Task × Window Radius × Filter × B)	56	(322.77)	

Note. Values enclosed in parentheses represent mean square errors. Cohen's *f* (dash) not calculated, as this is a nuisance variable.
* $p < .01$.

Table 3
Within-Subjects Analysis of Variance for Saccade Lengths as a Function of Task, Window Radius, and Peripheral Filtering Level

Source	*df*	*F*	Cohen's *f*
Blocks (B)	1	973.57*	—
Error (B)	14	(1.34)	
Task × B	1	2.78	0.08
Error (Task × B)	14	(0.16)	
Window Radius × B	2	15.84*	0.33
Error (Window Radius × B)	28	(0.18)	
Filter × B	2	25.31*	0.42
Error (Filter × B)	28	(0.18)	
Task × Window Radius × B	2	2.65	0.11
Error (Task × Window Radius × B)	28	(0.10)	
Task × Filter × B	2	1.38	0.05
Error (Task × Filter × B)	28	(0.14)	
Window Radius × Filter × B	4	0.30	0.00
Error (Window Radius × Filter × B)	56	(0.17)	
Task × Window Radius × Filter × B	4	0.15	0.00
Error (Task × Window Radius × Filter × B)	56	(0.11)	

Note. Values enclosed in parentheses represent mean square errors. Cohen's *f* (dash) not calculated, as this is a nuisance variable.
* $p < .01$.

As in the other analyses, window radius also had a clear effect on saccade length, which did not interact with level of peripheral filtering. However, in contrast to the other analyses, there was also a significant main effect and a large effect size (Cohen's $f = 0.42$) for peripheral filtering level. As before, we made planned comparisons between the full high-resolution control condition and all other Window Radius × Peripheral Filtering Level conditions. Figure 6 shows these comparisons as 95% confidence intervals for the difference between each of these conditions and the control; all of the conditions differed significantly from the control except Filtering Level 7 at the largest window radius (4.1°).

A comparison of Figures 5 and 6 shows that under the same circumstances and with the same number of observations, two filtering conditions (Levels 1 and 4 at a window radius of 4.1°) that did not differ significantly from the control for fixation durations, did differ from the control for saccade lengths. These findings suggest that the system controlling where the eyes move may be more sensitive to levels of peripheral filtering than the system controlling when the eyes move.

We also carried out a response-surface analysis on the mean saccade length data. In this analysis, we included five window radii (0°, 1.6°, 2.9°, 4.1°, and 21.6°) and four peripheral filtering–resolution levels (13, 7, 4, and 1 wavelet subbands) in 17 combinations. To our previously analyzed three window radii, we added two radii, 0° (an infinitely small window) and 21.6° (the hypotenuse of our 18° × 12° display, for our largest possible window). To our previously analyzed three levels of peripheral filtering resolution, we added a level having 13 subbands (our maximum resolution condition). The data for these additional levels in our analysis came from our constant high-resolution control condition, which can be viewed as having either an infinitely small window radius with maximum resolution outside of it or as a maximum sized window (extending beyond the image boundaries) with any of our levels of peripheral resolution outside of it. In this way, we were able to use our control condition data to represent the boundary conditions in our model.

We then explored the fit of a large number of potential equations to the data and found that the best-fitting equations were transition functions that are additive, with synergy and an intercept, such as the Gaussian cumulative function shown in Figure 7 ($R^2 = 0.98$, *df* adjusted $R^2 = 0.96$, fit $SE = 0.05$). This nonlinear function includes eight parameters: an x term having three parameters ($b = 1.0016$, $c = 3.5678$, $d = 2.2104$), a y term having three parameters ($e = 1.0080$, $f = 5.8556$, $g = 2.8897$), an interaction term that adds an additional parameter ($h = -0.9848$), and an intercept parameter ($a = 1.5529$). Note that the three parameters each in the x and y terms are the minimum needed for a nonlinear

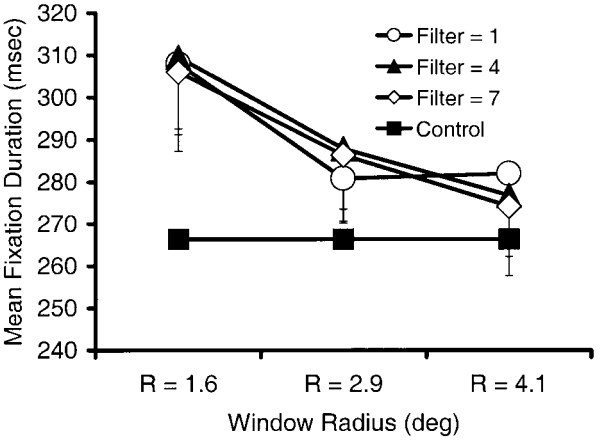

Figure 5. Mean fixation durations in milliseconds (msec) as a function of window radius, in degrees visual angle and filtering resolution level. R = the window radius, in degrees of visual angle (deg); Filter = filtering resolution level measured as number of wavelet subbands used in the wavelet reconstruction out of a total of 13, with fewer subbands resulting in lower resolution. Error bars represent 95% confidence intervals (two-tailed) for the difference of each experimental condition versus the full high-resolution control condition (Control).

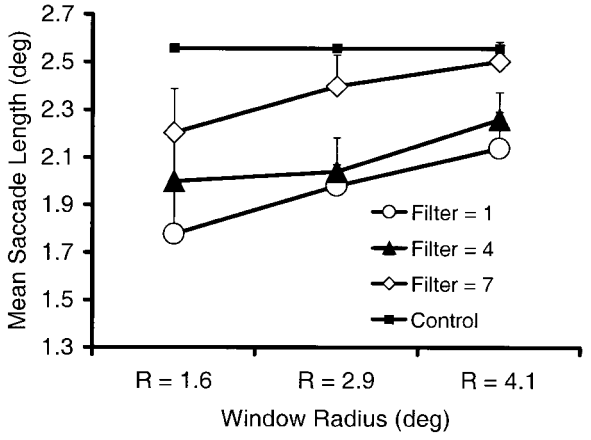

Figure 6. Mean saccade length in degrees visual angle as a function of window radius, in degrees visual angle and filtering resolution level. R = the window radius, in degrees of visual angle (deg); Filter = filtering resolution level measured as number of wavelet subbands used in the wavelet reconstruction out of a total of 13, with fewer subbands resulting in lower resolution. Error bars represent 95% confidence intervals (two-tailed) for the difference of each experimental condition versus the full high-resolution control condition (Control).

equation. Including additivity in the equation allows the window radius and filtering level axes to each form a different curve, and the interaction term allows the function to include a flat surface between these two axes. This flat region is one of the most important attributes of the function because it represents the set of image resolution and window radius combinations having no effect on the saccade target selection system, with all possible combinations in this range being equivalent. Adding the intercept constrains the function to converge to 0,0 on the window radius and filtering level axes at a point slightly lower than the minimum mean saccade length. The 0,0 point represents an image that is all middle gray (i.e., an infinitely small high-resolution window surrounded by a filtering level with zero information). Having the function converge to a mean saccade length slightly shorter than the minimum observed value seems reasonable, but is an extrapolation from the data, and is thus treated with caution. Specifically, the extrapolated origin represents eye movements on a completely even-gray screen, which would make the search and memory tasks impossible and would likely make eye movements less systematic than we find for our observed levels of filtering and window radii.

Another important feature of this function is its moderately steep saccade length growth rate, which predicts that for window radii greater than 10°, even our lowest peripheral resolution condition, Filtering Level 1, would produce saccade lengths no different from those with a full high-resolution image. This supposition, nonetheless, is based on interpolation and requires validation through further testing. Furthermore, we must qualify our interpretations regarding the filtering level axis. In particular, because of the unique characteristics of wavelet subband coding mentioned earlier in the *Stimuli* section, the only interpolated filtering level in the range of 1–13 that should be understood in terms of the number of wavelet subbands included in an image is Level 10. All other interpolated filtering levels in this range should be regarded as generalized resolution levels. Interestingly, the predicted mean saccade lengths for Filtering Level 10 show little effect for window radius, as we predicted on the basis of our earlier detection results.

Correlations between eye movement measures and search times. Table 4 reports the correlations among total fixations per trial, mean fixation durations and saccade lengths per trial, and $\log_{10}$

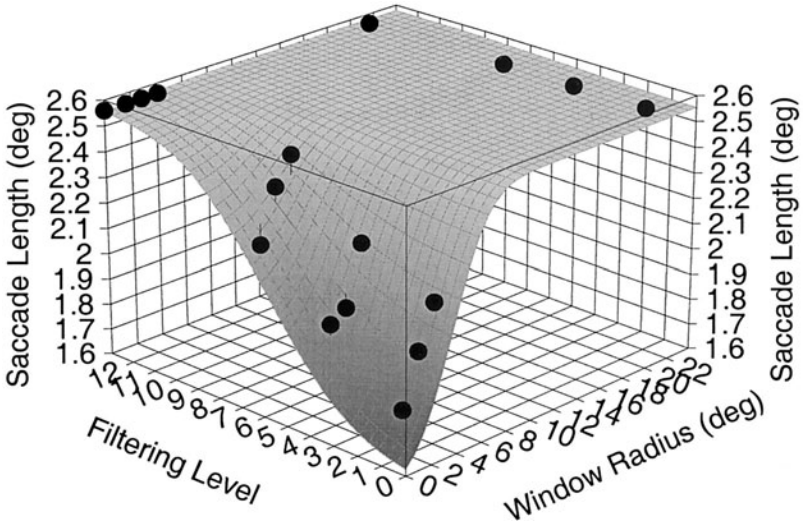

Figure 7. Saccade length response surface as a function of window radius, in degrees visual angle and filtering resolution level, fit to a Gaussian cumulative additive equation with synergy and an intercept (z = a + GCUM *x* [b, c, d] + GCUM *y* [e, f, g] + GCUM *x* [h, c, d] × GCUM *y* [1, f, g]). Window radius is measured in degrees of visual angle (deg); Filtering Level = filtering resolution level measured as number of wavelet subbands used in the wavelet reconstruction out of a total of 13, with fewer subbands resulting in lower resolution; Saccade Length = mean saccade length in degrees of visual angle (deg).

Table 4
Intercorrelations Between Log_{10} Search Times and Eye Movement Measures in the Search Task

Measure	Mean total fixations	Mean saccade length	Mean fixation duration
Log_{10} search time	.85††	−.32††	.09†
Total fixations	—	−.31††	.01
Mean saccade length	—	—	−.11*

Note. All means are on a per trial basis, with correlations based on individual trials for participants. 441 trials were included in the analysis. * $p < .05$, two-tailed. † $p < .05$, one-tailed. †† $p < .001$, one-tailed.

transformed search times. As we predicted, longer search times involve making more fixations (each of which takes more time), shorter saccades (requiring more fixations to cover the same image space, and thus more time), and longer fixation durations (taking more time), and we therefore report one-tailed probabilities for these correlations. However, we had no a priori predictions as to the direction of the relationship between saccade lengths and fixation durations, which turned out to be inversely related, and we therefore report the two-tailed probability for this correlation.

As suggested by the above correlations, a linear regression analysis indicated that much of the variance in the search times could be accounted for by the number of fixations made ($R^2 = .72$, $p < .01$), with mean fixation durations and saccade lengths adding only 0.7% ($p < .01$) and 0.3% ($p < .05$) more explained variance, respectively. However, the significant negative correlation between saccade lengths and total fixations shown in Table 4 suggests a possible reason why saccade lengths add little explained variance to the above regression. When the total fixations variable is excluded from the regression, we find that mean saccade length by itself explains about 10% of the variance ($p < .01$), with mean fixation duration not significantly adding to this variance ($p > .05$). Thus, it appears that peripheral filtering does not primarily slow search time through a disruption of processing that increases fixation durations, but is related to processes that reduce saccade lengths. The search process requires that the pictorial space be explored until the eyes come close enough to the target that a saccade can be made to it and its identity confirmed. As noted above, shortening saccades should reduce the picture coverage of a given number of saccades, reducing the likelihood of finding the target and thus increasing the number of fixations required before achieving success, thereby lengthening search time. However, because mean saccade lengths explain only 9% of the variance in the total number of fixations, there must be other important processes invoked by peripheral filtering that affect total fixations and the search process. One likely possibility is that peripheral filtering makes it more difficult to peripherally identify the target object.

Summary. The analysis of mean total fixations per trial showed that a possible trend toward more fixations as the window radius became smaller was not statistically significant. The mean duration of fixations, however, did increase with smaller windows, but was less affected by the level of peripheral filtering resolution. This pattern of results is also consistent with that of the search time data. All three variables are affected by the retinal eccentricity of the filtering to a greater degree than the level of peripheral resolution itself, within the range of detectable filtering levels used in this study. It is also worth noting that fixation durations are affected not only by foveal processing but peripheral processing as well, as there was no foveal filtering condition.

Mean saccade lengths were reduced by filtering out higher spatial frequencies in the visual periphery. This finding is consistent with the idea that above-threshold filtering reduces the salience of objects or regions in a display. For saccade lengths, we found significant main effects for both window radius and filtering level, which is what we would expect because both retinal eccentricity and spatial frequency affect contrast thresholds (Figure 1). In modeling the response surface for this data, we found a good-fitting function that showed a flat region of the surface where image resolution and retinal eccentricity could be traded one for the other in producing control level performance, and in which saccade lengths dropped off toward a minimum as a function of either image resolution or retinal eccentricity. This response surface might be construed as a rough model of the effect of image filtering and eccentricity on visual salience, as measured by eye movements.

The above eye movement analyses also help explain the longer average search times found with smaller window radii. Part of the longer search times can be explained in terms of above-threshold filtering leading to shorter saccades, resulting in more fixations, thus lengthening the time needed to locate a peripheral target. Thus, the effects of above-threshold filtering on saccade lengths may have important performance consequences. It is also consistent with the claim that not only search times but also saccade lengths reflect the operation of attentional selection mechanisms in natural tasks. However, because the reduction in saccade lengths can only explain a part of the variance in search times, peripheral filtering must make search inefficient in other ways as well. One possibility is that above-threshold filtering reduces the viewer's ability to resolve peripheral details and therefore impairs peripheral object recognition, or perhaps even the ability to detect object boundaries, thus making search less efficient. An interesting question is the degree to which such localized difficulties in object perception might cause more global problems, such as reducing a viewer's ability to recognize contextual information that could activate knowledge useful in guiding both attention and the eyes toward locations where the target is likely to be found.

How Does Peripheral Filtering Affect Where the Eyes Are Sent?

As noted earlier, we found neither a significant main effect nor any significant interactions involving task in our analysis of saccade length means. However, we also compared the frequency distributions of the lengths of saccades in the experimental conditions for the search and memory tasks and found that they were significantly different, $\chi^2(23, N = 25{,}220) = 117.93$, $p < .01$. Interestingly, we also found a significant difference between tasks for the control-condition saccade length distributions in these two tasks, $\chi^2(23, N = 14{,}265) = 37.25$, $p < .05$. Although the distributions appear quite similar, small differences are detected with a test based on such a large sample size. Because the study was not concerned with task differences, and because the task variable was confounded with serial order of task, these differences were not further explored and their data were combined for the analyses that follow. In these analyses, we further investigate

the nature of the effects of peripheral resolution level and window radius in reducing mean saccade length and propose three possible explanations for such reductions: (a) The eyes are attracted to the window edge, (b) peripheral resolution has a general influence on saccade length, or (c) peripheral resolution produces local influences on saccade length.

Attraction to the window edge. Biresolutional images necessarily have a texture boundary between the higher and lower resolution regions. In the present case, this boundary was circular, with a near-equal retinal eccentricity in all directions for images in the same window radius condition. It is possible that the textural discontinuity at the window boundary attracted the gaze. This situation would produce an increase in the number of saccades of about the length of the window radius in each experimental condition, with this increase becoming larger with higher filtering levels that increase the discontinuity. The top graph in Figure 8 shows the relative frequency of saccades of different lengths in the control and experimental conditions, with data collapsed across peripheral filtering level. To clarify the impact of the experimental conditions relative to the control condition, the bottom graph in

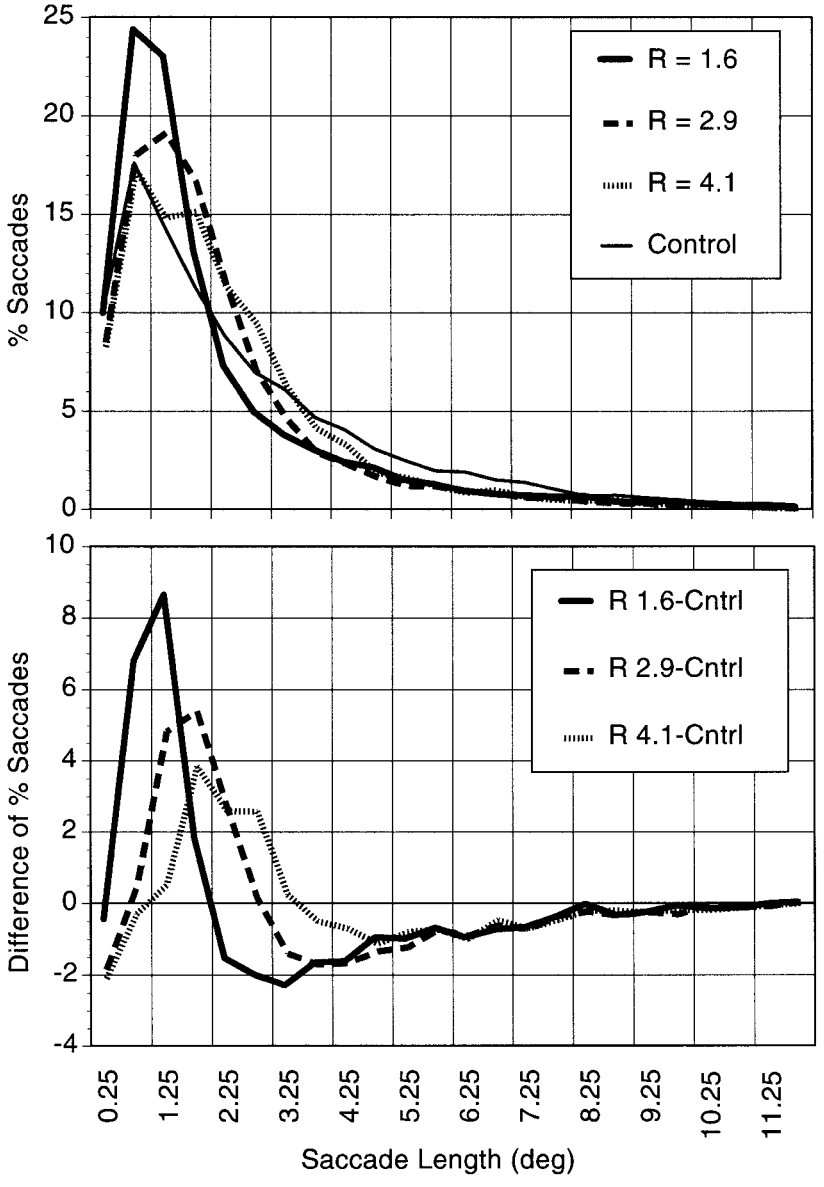

Figure 8. Relative frequency of saccades of different lengths as a function of window radius. Top graph shows the percentage of saccade lengths for each window radius condition versus the control condition. Bottom graph shows the difference between each radius condition and the control condition. Data represent the midpoints of bins 0.5° visual angle in width. R = the window radius, in degrees of visual angle (deg); Control = constant highest resolution image; R 1.6-Cntrl = difference between window radius of 1.6° and full high-resolution image; R 2.9-Cntrl and R 4.1-Cntrl = analogous difference measures for the 2.9° and 4.1° window radii.

Figure 8 plots the differences between the distributions for the control condition and each of the experimental conditions, showing the increase or decrease in the relative frequency of saccades for each retinal eccentricity. Although this graph clearly shows differences among the window radius conditions, there is no consistent increase in the relative frequency of saccades at the eccentricity corresponding to the window boundary in each condition. Although the smallest window does show a slight increase in the frequency of saccades in the 1.6° region (i.e., the 1.75° bin), the medium sized window shows no change in the frequency of saccades in the 2.9° region (the 2.75° bin), and the large window shows an actual reduction in the frequency of saccades in the 4.1° region (the 4.25° bin). Indeed, for all three conditions, the distance at which the peak increase in number of saccades occurs is considerably shorter than (41–45% of) the window radius distance. Thus, the data do not support the hypothesis that the eyes are attracted to the edge of the window.

There is, however, a possible explanation for why the peaks of the control-minus-experimental saccade length distributions are short of their respective experimental condition window radii. According to this argument, the window radius may not always correspond to the actual distance from the center of gaze to the window edge because of error in positioning the gaze-contingent window. An ideal GCMRD would always center the high-resolution window exactly at fixation. In the current study, however, our method involved selecting a biresolutional image from a set of 330 precomputed versions of the picture, based on eye position within an imaginary 22 × 15 grid. This method minimized image-updating time on each fixation, but also resulted in violating the ideal: Most fixations would not fall precisely on one of the grid points, and thus the high-resolution area would not be perfectly centered on fixation. Thus, the nearest edge of the window would be closer than the window radius, and, conversely, the farthest edge would be farther. Because grid points were 0.82° apart, the eyes could be as far as 0.41° from a grid point horizontally, or 0.57° diagonally, and still be assigned to that grid point, causing imperfect window placement. In addition, slight ocular motion at the start of a fixation might sometimes move the eyes from the grid point for the image version being displayed, thus further increasing the window placement error.

If the eyes were being drawn to the edge between the high- and low-resolution areas of the image, such window placement error might produce saccades shorter than the window radius. This would result in a peak in the control-minus-experimental saccade length distribution at a distance shorter than the window radius, as is observed in the data. This raises two questions. First, is the magnitude of the window placement error sufficient to account, potentially, for the observed discrepancy between the window radii and the peaks of the control-minus-experimental saccade length distributions? Second, is there any evidence that window placement error actually shortens saccades? To answer the first question, we determined the window placement error for each fixation. The window placement error distribution had a mode of 0.26°, a mean of 0.44°, and a standard deviation of 0.30°. These figures suggest that in two out of the three window conditions (2.9° and 4.1°), the magnitude of the observed window-positioning error was too small to account for the observed differences between the peaks of the control-minus-experimental saccade length distributions and the window radii. Only in the 1.6° window radius condition is the error large enough to potentially explain the shift in the peak based on the assumption that the eyes were being drawn to the window edge, if window placement error in fact shortens saccades.

To determine whether such error actually shortens saccades, we divided the eye fixations in each window radius condition among those having window placement error less than or greater than 0.4° (the median placement error), and then calculated the average length of the following saccades. Table 5 shows a two-way within-subjects ANOVA on mean saccade lengths as a function of the size of the preceding window placement error and window radius. Only window radius produced a statistically significant effect on saccade length.

Finally, we plotted the control-minus-experimental saccade length distributions for smaller and larger error cases for each window radius condition and found them to be very similar. If saccades were being shortened in the larger error cases, because of attraction to the closest edge of the window, this would result in fewer saccades of a length corresponding to the window radius compared with the smaller error cases. In contrast, two out of the three window radius conditions (1.6° and 2.9°) showed the opposite pattern, that is, a slightly higher relative frequency of saccades at the window radius length for the larger error cases than for the smaller error cases. Only the third radius condition (4.1°) showed the predicted pattern, though again the difference between window

Table 5
Within-Subjects Analysis of Variance for Saccade Lengths as a Function of Degree of Window Placement Error and Window Radius

Source	*df*	*F*	Cohen's *f*
Blocks (B)	1	1050.92*	—
Error (B)	14	(0.375)	
Window Error × B	1	1.41	0.07
Error (Window Error × B)	14	(8.66E-03)	
Window Radius × B	2	13.94*	0.54
Error (Window Radius × B)	28	(0.06)	
Window Error × Window Radius × B	2	3.14	0.22
Error (Window Error × Window Radius × B)	28	(0.01)	

Note. Values enclosed in parentheses represent mean square errors. Cohen's *f* (dash) not calculated, as this is a nuisance variable. The degree of window placement error is greater than or less than 0.4°.
* $p < .01$.

error conditions was slight. Thus, the discrepancy between the peaks of the control-minus-experimental saccade length distributions and their respective experimental-condition window radii cannot be explained by window placement error, and the hypothesis that the eyes are attracted to the window edge is unsupported.

General influence of peripheral resolution on saccade length. An alternative hypothesis is that above-threshold filtering in the periphery generally disrupts saccadic activity. Because we know that mean saccade length is shortened by above-threshold filtering, the simplest model would predict a general proportional shortening of all saccades, with greater shortening caused by a smaller window radius and lower peripheral resolution. This hypothesis can be evaluated by examining Figures 8 and 9. Figure 9 shows the relative frequency of different saccade lengths in the control and each peripheral-filtering resolution condition, collapsed across window radii. This graph shows that as peripheral resolution decreases, the relative frequency of longer saccades decreases, which is consistent with the general disruption hypothesis. However, two pieces of evidence run counter to this hypothesis. First, if decreasing resolution shortened all saccades, then there should be an increase in the relative proportion of the shortest saccade lengths. In fact, Figure 9 shows a decrease in the frequency of the shortest saccades with decreasing peripheral resolution. Second, when a distribution is compressed, as when all saccades are shortened, the new distribution must cross the control distribution at some point. If there were a general proportional shortening of all saccades with decreasing resolution, we should find the crossing point moving leftward with decreasing resolution as saccades are further shortened. However, as shown in the bottom graph of Figure 8, the crossing point is essentially the same for all three resolution conditions, occurring in the 2.75° bin region, that is, the bin corresponding to the average window radius used in the study (2.87°). Therefore, it seems unlikely that above-threshold peripheral filtering generally shortens all saccades.

Local influences of peripheral resolution on saccade length. The pattern of the data is most harmonious with the third hypothesis, which posits more local effects on saccade length, though without drawing the eyes to the window boundary region. A simple model of such local influences assumes that, for each saccade, there are many candidate targets from among which one is selected through a *winner-take-all* competition (Findlay & Walker, 1999; Itti & Koch, 2000; Koch & Ullman, 1985; Sheinberg & Zelinsky, 1993). In this competition, objects that are above-threshold filtered do not compete as well as those that are high-resolution or below-threshold filtered. Thus, when an object that would normally win fails to do so because it is above-threshold filtered, some object in the high-resolution area is more likely to win. The result should be relatively fewer saccades longer than the window radius distance, and thus more saccades shorter than this distance, with a crossing point relative to the control condition near the window radius value.

Figures 8 and 9, which collapse across levels of filtering, are quite compatible with this explanation. Each of the curves in the top graph of Figure 8 crosses the control condition (and reaches zero in the bottom graph) close to the window radius for that experimental condition, having relatively fewer saccades than does the control condition beyond the window radius, and relatively more saccades within the window region. This decreased likeli-

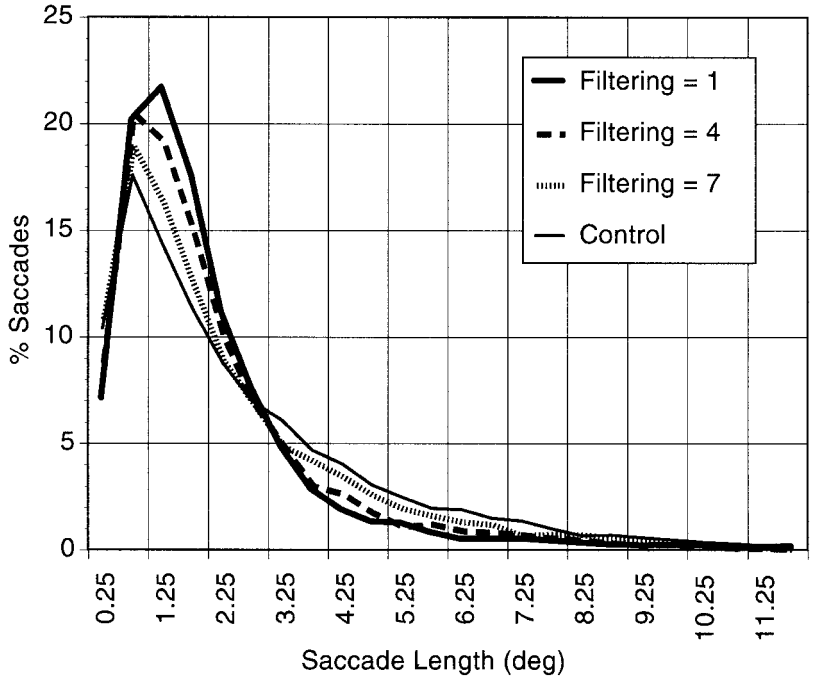

Figure 9. Relative frequency distributions of saccade lengths as a function of filtering resolution level. Data represent the midpoints of bins 0.5° visual angle in width. Filtering = filtering resolution level measured as number of wavelet subbands used in the wavelet reconstruction out of a total of 13, with fewer subbands resulting in lower resolution; Control = constant highest resolution image; deg = degrees of visual angle.

hood of making saccades beyond the edge of the high-resolution window is what we would expect based on the local saliency hypothesis, because above-threshold filtering only exists outside the window.

The local saliency hypothesis can be extended to assume that when the visual periphery is filtered at an above-threshold level, changes in saliency and resolution are positively correlated: As resolution decreases, so too does saliency. This correlation leads, first, to the prediction that, with filtering level held constant, there should be no difference among window radius conditions in length-specific saccade frequencies in the region beyond the largest window radius. We make this prediction because, in this region, the change in resolution, compared with the control condition, is the same for all window radius conditions. Figure 8 confirms this prediction; the bottom graph shows very similar saccade length frequencies among conditions beyond 4.1°. To statistically test the prediction, we carried out a two-way within-subjects ANOVA in which the dependent measure was the difference between relative frequencies of saccade lengths in each of the window radius conditions (collapsed across filtering level) versus the control condition, for each of the 15 bins greater than the 4.25° bin. Table 6 reports the results: The window radius factor was not significant. There was, of course, a significant effect for the binned saccade length factor, because the relative frequencies of saccades decrease with eccentricity in all window radius conditions. More important, the interaction between window radius and binned saccade length was not significant (observed power at $p = .05$ was 0.56).

A second prediction arises from the difference between the constant level of filtering outside the window and the continuous drop-off of visual resolution with retinal eccentricity. Suppose a given level of filtering reduces the saliency of objects at a given eccentricity because it removes information that would otherwise have been salient. At some further eccentricity, however, the same level of filtering should have no effect on the saliency of objects because the same critical information would no longer be resolvable by the visual system even without peripheral filtering. Thus, across levels of filtering, the reduction in length-specific saccade frequencies just beyond the window radius should be greatest for the smallest window and least for the largest window. The bottom graph of Figure 8 clearly shows this pattern.

A third prediction is that with increasingly excessive filtering, there should be reduced levels of saliency. We tested this prediction with a two-way within-subjects ANOVA, shown in Table 7, similar to that reported above, with saccade-frequency difference data for the 15 bins beyond the 4.25° bin, but with peripheral filtering level, collapsed across window radii, as the first factor. This was done to test, in peripheral regions that were filtered in all conditions, whether saliency changes (here measured as drops in length-specific saccade frequencies) varied with level of filtering. The results showed statistically significant effects for filtering resolution level, binned saccade length, and the interaction between these two factors. Thus, increasing the level of filtering in the visual periphery reduces the saliency of peripheral objects, as indicated by a reduced likelihood of the eyes leaving the high-resolution window. These effects are all consistent with the local saliency hypothesis and the competition model of saccade target selection.

To extend this local competition model, it is necessary to explain where shortened saccades tend to go. The simplest assumption is that the control condition saccade-length relative frequency distribution represents the saliency distribution for candidate objects within the high-resolution area, whatever its size. From this assumption, two inferences follow. First, there are saccades that would have gone to objects within the window region regardless of the peripheral filtering outside the window, and the probability of sending the eyes to these objects is equal to the control condition probabilities at each distance less than a given window radius. Second, there are some saccades that would have gone to objects outside the window but, because of the reduced saliency of those objects in the experimental conditions, are attracted instead to objects within the window. Because the control condition data indicate the saliency distribution within the window, as above, these shortened saccades should also be distributed according to this distribution. The implication of this assumption is that saccade length frequency distributions within the window area for each experimental condition should be similar in shape to that in the control condition, with just a proportional increase in the number of saccades of each length that varies with condition.

If this prediction were accurate, the experimental-minus-control curves in the bottom graph in Figure 8 for saccades shorter than the radius should be flat and positive, because of an equivalent in-

Table 6
Within-Subjects Analysis of Variance for Difference Between Experimental and Control Relative Frequency of Saccades Beyond All Window Radii as a Function of Window Radius and Retinal Eccentricity

Source	*df*	*F*	Cohen's *f*
Blocks (B)	1	124.51*	—
Error (B)	14	(1.19E-04)	
Window Radius × B	2	0.78	0.00
Error (Window Radius × B)	28	(3.32E-05)	
Eccentricity × B	4.00[a]	11.00*	0.46
Error (Eccentricity × B)	56.06[a]	(2.14E-04)	
Window Radius × Eccentricity × B	6.62[a]	1.42	0.13
Error (Window Radius × Eccentricity × B)	92.63[a]	(5.53E-05)	

Note. Values enclosed in parentheses represent mean square errors. Cohen's *f* (dash) not calculated, as this is a nuisance variable.
[a] Box epsilon corrected degrees of freedom.
* $p < .01$.

Table 7
Within-Subjects Analysis of Variance for Difference Between Experimental and Control Relative Frequency of Saccades Beyond All Window Radii as a Function of Peripheral Filtering Level and Retinal Eccentricity

Source	*df*	*F*	Cohen's *f*
Blocks (B)	1	125.71*	—
Error (B)	14	(1.18E-04)	
Filtering × B	1.40[a]	39.93*	0.34
Error (Filtering × B)	19.55[a]	(4.99E-05)	
Eccentricity × B	4.07[a]	11.20*	0.46
Error (Eccentricity × B)	57.01[a]	(2.09E-04)	
Filtering × Eccentricity × B	6.40[a]	4.95*	0.40
Error (Filtering × Eccentricity × B)	89.55[a]	(6.06E-05)	

Note. Values enclosed in parentheses represent mean square errors. Cohen's *f* (dash) not calculated, as this is a nuisance variable.
[a] Box epsilon corrected degrees of freedom.
* $p < .01$.

crease relative to the control distribution at all eccentricities within the window. Yet, the curves peak at different locations for the different window size conditions and show a negative proportion change for the shortest saccades, thus failing to support the simple saccade redistribution model just proposed. It appears that biasing factors are changing the saccade length distribution for shortened saccades. These biases lead to peaks in the experimental-minus-control saccade length distributions that are at greater eccentricities than that of the peak in the control distribution. Another challenge to our assumption that saccades inside the window should mirror the condition distribution is that the frequencies of the shortest saccades in the experimental conditions are below those of the control condition (bottom of Figure 8), even though there is an increase in the number of saccades remaining in the window region. The basis for these changes in distribution require further investigation.

Summary. Above-threshold peripheral filtering shortens viewers' mean saccade lengths. This shortening appears to be due neither to a tendency for the texture discontinuity at the edge of the high-resolution window to draw the eyes nor to a tendency for the presence of above-threshold peripheral filtering to produce a general shortening of all saccades. Rather, the influences are more local, with relatively fewer saccades going into the filtered region, and, instead, with more saccades going into the high-resolution area. A simple model that assumes a competition among potential saccade targets, with above-threshold filtering reducing objects' relative salience, can account for the reduced relative frequency of saccades in the filtered region. It cannot, however, account for where these shortened saccades tend to go in the high-resolution window: the landing positions of these saccades tend to be more distant than those of the assumedly unaffected saccades.

How Does Peripheral Filtering Affect When the Eyes Leave?

The above discussion suggests that there may be different classes of saccades in the experimental conditions: Type 1, saccades that go outside the window in spite of the peripheral filtering; Type 2, saccades that remain in the window area; and Type 3, saccades that would have gone outside the window but instead were sent within the window because of the peripheral filtering. (A fourth possibility, saccades that would otherwise have stayed within the window but are drawn into the filtered area, is not considered because there is no evidence that they occur.) Type 1 saccades are those that go outside the window in experimental conditions. Saccades that go to locations within the window are a combination of Type 2 and Type 3. The proportion of saccades sent to locations within a specified window radius in the control condition gives an estimate of the proportion of Type 2 saccades in an experimental condition, whereas the difference between the proportion of saccades going to this region in the experimental and control conditions indicates the proportion of Type 3 saccades. A question to consider is: Are there differences in fixation duration preceding these three different types of saccades?

There are at least three possible effects relating the duration of a fixation to the type of saccade that follows it: (a) a general effect in which above-threshold peripheral filtering disturbs processing and increases the durations of all fixations, (b) an effect limited only to fixations preceding saccades that are redirected from distant to closer areas, or (c) an effect that is related to hypothesized dynamics of competition in selecting a target object. The first possibility predicts no differences in fixation durations as a function of the three types of following saccades. In the second possibility, only redirected saccades (Type 3) are preceded by longer fixations. This would predict average fixation durations prior to saccades sent into the filtered periphery (all Type 1), but longer than average fixation durations preceding saccades keeping the eyes within the window region (some Type 3). The third possibility requires predictions on the basis of assumptions about how reduced salience of peripheral regions influences the time to resolve the competition for selecting the next saccade target. For example, when the salience of peripheral objects is reduced and these objects therefore exert less influence on the competition, the fixation durations preceding Type 2 saccades might also be reduced, thus suggesting the possibility of shorter fixations when the eyes remain within the window.

Figure 10 presents the mean fixation durations prior to saccades of different lengths in the three window radius and control conditions. To maintain equivalent stability of both fixation duration and

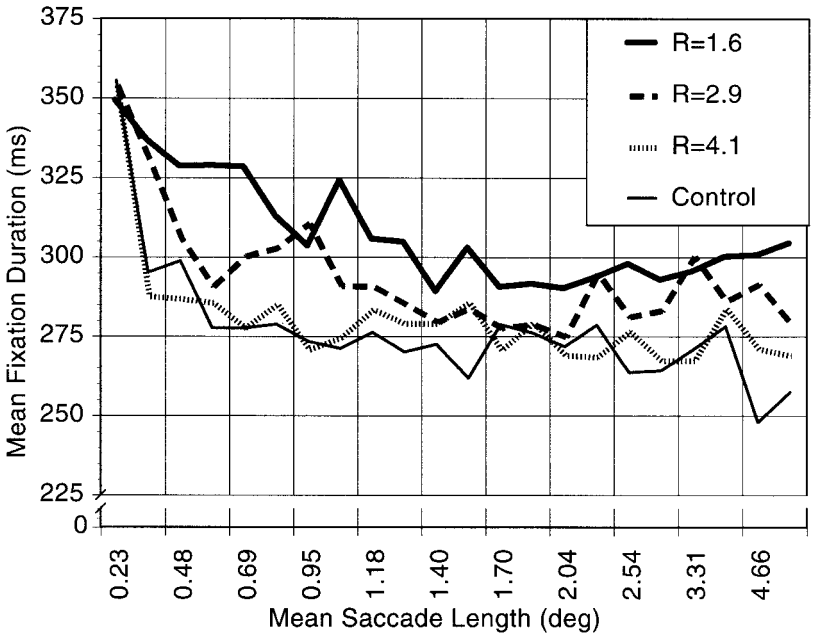

Figure 10. Mean fixation durations in milliseconds as a function of following mean saccade length and window radius, both in degrees visual angle. R = the window radius, in degrees of visual angle (deg); Control = constant highest-resolution image; ms = milliseconds.

saccade length data, the following procedures were used. Saccades were rank ordered by length and put in bins of 300 ± 15 cases. For each bin, we calculated the mean saccade length and calculated the mean duration of fixations preceding those saccades separately for each window radius condition across filtering levels, with an attempt to select bins having nearly equivalent mean saccade lengths in the different window conditions. The average bin size was 0.1°.

Figure 10 indicates that fixation durations in the two smallest window radius conditions are elevated relative to the control prior to saccades of all lengths except the shortest (0.23°). Fixations in the 4.1° radius condition are similar in duration to those of the control condition at all saccade lengths. Thus, fixation durations are unaffected by whether they are followed by saccades sent either inside or outside the window in each radius condition. Hence, the data indicate that the presence of above-threshold peripheral filtering has a generally disruptive effect on processing, sparing only the fixations before the shortest saccades. Whether the disruption occurs at low-perceptual and eye movement control levels, or results from higher cognitive levels, such as a reduced ability to gain information about the content of the image to guide attention to task-relevant areas, is an issue requiring further study.

Thus, although above-threshold filtering has local effects on saccade target selection, as shown by its influence on saccade lengths, the effect on fixation durations appears to be more global, presumably reflecting a general impact on processing.

SUMMARY AND CONCLUSIONS

We investigated the effects of peripheral spatial filtering on search-task performance and eye movements during free viewing through use of a fast, gaze-contingent, multiresolutional display, with normal spatial frequency content at the point of gaze and reduced higher spatial frequencies in the periphery. This method allowed us to investigate issues central to both spatial vision and attention by using naturalistic stimuli, tasks, presentation conditions, and measures. In particular, we considered whether the current understanding of eccentricity-dependent contrast sensitivity functions can be extended to the realm of attentional selection, and at the same time scaled up to more naturalistic conditions. This study tested the hypothesis that high spatial frequency information contributes to the salience of objects, in terms of their likelihood of attracting the eyes during free viewing.

Our results showed that the window radius, that is, the retinal eccentricity at which filtering begins, affected search times, saccade lengths, fixation durations, and possibly total fixations as well, suggesting that both attentional selection and visual processing are affected by the spatial frequency contents of the visual periphery. We suggest that the reduced salience and/or recognizability of peripheral targets by above-threshold filtering may, in part, explain why smaller windows cause longer search times. Reducing objects' salience, recognizability, or both would result in making shorter saccades, which, in order to scan a given image for the target, would necessitate making more total fixations, and thus lengthen the search time.

We expected that both window radius and the range of filtered spatial frequencies would affect image scanning, and this effect was most clearly shown in saccade target selection, as indicated by changes in saccade length. Three possible explanations for these saccade length results were considered: (a) the eyes are drawn to the discontinuity at the boundary of the high-resolution window and the filtered area, (b) peripheral filtering generally disrupts saccade programming, or (c) peripheral filtering reduces the probability that an object would win a saliency competition for atten-

tional and saccade target selection. The data support the third explanation, with the eyes going less frequently to peripheral locations where high spatial frequencies are attenuated, and thus going more frequently to locations in the high-resolution window. A more complete model of such a saliency competition would also predict where in the high-resolution window such saccades are redistributed. We rejected a hypothesis that the shortened saccades would have landing positions distributed according to the relative salience of objects in that region, as indicated by the control condition; the shortened saccades tended to be redistributed among more distant locations within the unfiltered region than those in the control condition—symmetrically centered between the point of gaze and the window radius. However, an adequate explanation for this redistribution requires further research.

We also investigated the related issue of the link between saccade targeting and fixation durations. We proposed three hypotheses regarding this relationship: (a) fixations preceding saccades sent into the filtered periphery would, on average, be longer, because of the decreased salience of those targets and the increased salience of targets within the window; (b) fixations preceding saccades sent to targets inside the window would, on average, be longer, because of reprogramming saccades originally targeted to peripheral objects; (c) fixations in above-threshold filtering conditions would, on average, be longer regardless of the length of the following saccade, because of a general disruption of processing. We found that, for all saccade lengths except the shortest, average fixation durations were greater in the smaller window conditions. This finding is inconsistent with either the competition or saccade redirection hypotheses and suggests that the effects of above-threshold filtering on saccade targeting and fixation durations are independent, a reasonable assumption if the process of selecting targets for attention works on the basis of some sort of race model. Then, rather than lengthening the time to program a saccade, the presence of above-threshold filtering in the visual periphery may simply increase the likelihood of selecting a target within the higher resolution window. Together, these two sets of assumptions could explain our results. Nevertheless, this issue deserves further consideration.

Our findings also have clear practical significance. GCMRDs are particularly useful for image compression in single-user displays with limited transmission bandwidth needing both high resolution and fast update rates. These include video telephony, telemedicine, teleoperation, and remote piloting (Geisler & Perry, 1998, 1999; for review see Reingold et al., in press). By using GCMRDs, a constant resolution image can be transmitted progressively, sending only a small part of the image in high resolution where the viewer is looking at a given moment, with lower resolution information everywhere else (Frajka, Sherwood, & Zeger, 1997; To, Lau, & Green, 2001; Wang & Bovik, 2001). Wavelet filtering is particularly appropriate for this purpose because the representations are complete yet sparse (Moulin, 2000), and, because of their hierarchical structure, can be truncated at any point by the sender and still yield an acceptable image at the decoding stage (Wang & Bovik, 2001). For these reasons, we used one of the most commonly used wavelet filters, the 9/7 biorthogonal, to produce our biresolutional images.

The current study contributes to the development of such wavelet-based progressive transmission systems by providing data on the effects of wavelet filtering on performance and eye measures, as well as providing a model of effects on saccade lengths as a function of retinal eccentricity and the number of wavelet subbands used in the filtered image (see Figure 7). Thus, we provide complementary information, linking perception and action, to designers who have more commonly used visual sensitivity measures in constructing multiresolutional image transmission systems (Duchowski, 2000; Geisler & Perry, 1998; Wang & Bovik, 2001). Future studies comparing the effects of GCMRD parameters on such an array of perception and performance measures are clearly needed.

More generally, the current study suggests that above-threshold peripheral filtering can impair task performance, such as visual search, caused, in part, by a sort of tunnel vision, measured in terms of reduced saccade lengths. The function in Figure 7, although needing further validation, provides testable predictions for a range of Window Radius $\times$ Filtering Level combinations that should produce normal eye movement behavior. However, if one wants to focus a viewer's attention within a given region, for example in a virtual environment, peripheral image filtering may turn out to be a useful means of doing so, by making objects in the high-resolution area relatively more salient than they otherwise would have been. Further studies are needed to determine more precisely the spatial frequency filtering cut-offs at given retinal eccentricities that result in the types of effects we have reported and the functional basis of these saliency effects.

Finally, we concede that our GCMRD system had very high spatial and temporal resolution, and would not likely be matched by most systems used in applied settings, at least for some time. Thus, studies are needed to investigate how the effects of stimulus parameters such as retinal eccentricity and peripheral resolution level vary as a function of the spatial and temporal resolution of the GCMRD systems used.

References

Anderson, S. J., Mullen, K. T., & Hess, R. F. (1991). Human peripheral spatial resolution for achromatic and chromatic stimuli: Limits imposed by optical and retinal factors. *Journal of Physiology (Lond), 442,* 47–64.

Antonini, M., Barlaud, M., Mathieu, P., & Daubechies, I. (1992). Image coding using wavelet transform. *IEEE Transactions on Image Processing, 1,* 205–220.

Banks, M. S., Sekuler, A. B., & Anderson, S. J. (1991). Peripheral spatial vision: Limits imposed by optics, photoreceptors, and receptor pooling. *Journal of the Optical Society of America, 8,* 1775–1787.

Boff, K. R., & Lincoln, J. E. (1988). *Engineering data compendium—Human perception and performance* (Vol. III). Wright-Patterson, OH: Armstrong Aerospace Medical Research Laboratory.

Burr, D. C., Morrone, M. C., & Ross, J. (1994, October 6). Selective suppression of the magnocellular visual pathway during saccadic eye movements. *Nature, 371,* 511–513.

Cannon, M. W. (1985). Perceived contrast in the fovea and periphery. *Journal of the Optical Society of America, 2,* 1760–1768.

Colby, C. L., & Goldberg, M. E. (1999). Space and attention in parietal cortex. *Annual Review of Neuroscience, 22,* 319–349.

Deubel, H. (1991). Eye movements as a probe into preattentive visual processing. *Perception, 20,* A54.

Deubel, H., & Schneider, W. X. (1996). Saccade target selection and object recognition: Evidence for a common attentional mechanism. *Vision Research, 36,* 1827–1837.

Duchowski, A. T. (2000). Acuity-matching resolution degradation through wavelet coefficient scaling. *IEEE Transactions on Image Processing, 9,* 1437–1440.

Findlay, J., & Walker, R. (1999). A model of saccade generation based on parallel processing and competitive inhibition. *Behavioral and Brain Sciences, 22,* 661–721.

Frajka, T., Sherwood, P. G., & Zeger, K. (1997). Progressive image coding with spatially variable resolution. *Proceedings of the International Conference on Image Processing,* 53–56.

Geisler, W. S., & Perry, J. S. (1998). A real-time foveated multi-resolution system for low-bandwidth video communication. *Proceedings of the SPIE: The International Society for Optical Engineering, 3299,* 294–305.

Geisler, W. S., & Perry, J. S. (1999). Variable-resolution displays for visual communication and simulation. *The Society for Information Display, 30,* 420–423.

Gottlieb, J. P., Kusunoki, M., & Goldberg, M. E. (1998, January 29). The representation of visual salience in monkey parietal cortex. *Nature, 391,* 481–484.

Hoffman, J. E., & Subramaniam, B. (1995). The role of visual attention in saccadic eye movements. *Perception & Psychophysics, 57,* 787–795.

Irwin, D. E., Colcombe, A. M., Kramer, A. F., & Hahn, S. (2000). Attentional and oculomotor capture by onset, luminance, and color singletons. *Vision Research, 40,* 1443–1458.

Irwin, D. E., & Gordon, R. D. (1998). Eye movements, attention and trans-saccadic memory. *Visual Cognition, 5,* 127–155.

Issa, N. P., Trepel, C., & Stryker, M. P. (2000). Spatial frequency maps in cat visual cortex. *Journal of Neuroscience, 20,* 8504–8514.

Itti, L., & Koch, C. (2000). A saliency-based search mechanism for overt and covert shifts of visual attention. *Vision Research, 40,* 1489–1506.

Itti, L., & Koch, C. (2001). Computational modeling of visual attention. *Nature Reviews Neuroscience, 2,* 194–203.

Julesz, B. (1981, March 12). Textons, the elements of texture perception, and their interactions. *Nature, 290,* 91–97.

Kirk, R. E. (1995). *Experimental design: Procedures for the behavioral sciences* (3rd ed.). Pacific Grove, CA: Brooks/Cole.

Koch, C., & Ullman, S. (1985). Shifts in selective visual attention: Towards the underlying neural circuitry. *Human Neurobiology, 4,* 219–227.

Kowler, E., Anderson, E., Dosher, B., & Blaser, E. (1995). The role of attention in the programming of saccades. *Vision Research, 35,* 1897–1916.

Krieger, G., Rentschler, I., Hauske, G., Schill, K., & Zetzsche, C. (2000). Object and scene analysis by saccadic eye-movements: An investigation with higher-order statistics. *Spatial Vision, 13,* 201–214.

Kustov, A. A., & Robinson, D. L. (1996, November 7). Shared neural control of attentional shifts and eye movements. *Nature, 384,* 74–77.

Loschky, L. C., & McConkie, G. W. (2000). User performance with gaze contingent multiresolutional displays. In A. T. Duchowski (Ed.), *Proceedings of the Eye Tracking Research & Applications Symposium 2000* (pp. 97–103). Palm Beach, FL: Association of Computing Machinery.

Mannan, S., Ruddock, K. H., & Wooding, D. S. (1995). Automatic control of saccadic eye movements made in visual inspection of briefly presented 2-D images. *Spatial Vision, 9,* 363–386.

Mannan, S. K., Ruddock, K. H., & Wooding, D. S. (1997). Fixation patterns made during brief examination of two-dimensional images. *Perception, 26,* 1059–1072.

McConkie, G. W., & Loschky, L. C. (2002). *Perception onset time during fixations in free viewing.* Manuscript submitted for publication.

Moraglia, G. (1989). Visual search: Spatial frequency and orientation. *Perceptual & Motor Skills, 69,* 675–689.

Motter, B. C., & Belky, E. J. (1998). The guidance of eye movements during active visual search. *Vision Research, 38,* 1805–1815.

Moulin, P. (2000). Multiscale image decompositions and wavelets. In A. C. Bovik (Ed.), *Handbook of image and video processing* (pp. 289–300). New York: Academic Press.

Niu, E. L.-C. (1995). *Gaze-based video compression using wavelets.* Unpublished master's thesis, University of Illinois at Urbana–Champaign, Urbana.

Peli, E., & Geri, G. A. (2001). Discrimination of wide-field images as a test of a peripheral-vision model. *Journal of the Optical Society of America A-Optics & Image Science, 18,* 294–301.

Peli, E., Yang, J., & Goldstein, R. B. (1991). Image invariance with changes in size: The role of peripheral contrast thresholds. *Journal of the Optical Society of America, 8,* 1762–1774.

Pointer, J. S., & Hess, R. F. (1989). The contrast sensitivity gradient across the human visual field: With emphasis on the low spatial frequency range. *Vision Research, 29,* 1133–1151.

Reinagel, P., & Zador, A. M. (1999). Natural scene statistics at the centre of gaze. *Network-Computation in Neural Systems, 10,* 341–350.

Reingold, E. M., Loschky, L. C., McConkie, G. W., & Stampe, D. M. (in press). *Gaze-contingent multi-resolutional displays: An integrative review. Human Factors.*

Robson, J. G., & Graham, N. (1981). Probability summation and regional variation in contrast sensitivity across the visual field. *Vision Research, 21,* 409–418.

Sagi, D. (1988). The combination of spatial frequency and orientation is effortlessly perceived. *Perception & Psychophysics, 43,* 601–603.

Schall, J. D., & Bichot, N. P. (1998). Neural correlates of visual and motor decision processes. *Current Opinion in Neurobiology, 8,* 211–217.

Schall, J. D., Hanes, D. P., Thompson, K. G., & King, D. J. (1995). Saccade target selection in frontal eye field of Macaque: I. Visual and premovement activation. *Journal of Neuroscience, 15,* 6905–6918.

Sekuler, R., & Blake, R. (2002). *Perception.* (4th ed.). New York: McGraw-Hill.

Sheinberg, D. L., & Zelinsky, G. J. (1993). A cortico–collicular model of saccadic target selection. In G. d'Ydewalle & J. V. Rensbergen (Eds.), *Perception and cognition: Advances in eye movement research* (Vol. 4, pp. 333–348). Amsterdam: North-Holland/Elsevier.

Shioiri, S., & Cavanagh, P. (1989). Saccadic suppression of low-level motion. *Vision Research, 29,* 915–928.

Shioiri, S., & Ikeda, M. (1989). Useful resolution for picture perception as a function of eccentricity. *Perception, 18,* 347–361.

Silverman, M. S., Grosof, D. H., De Valois, R. L., & Elfar, S. D. (1989). Spatial-frequency organization in primate striate cortex. *Proceedings of the National Academy of Sciences, USA, 86,* 711–715.

Thompson, K. G., Bichot, N. P., & Schall, J. D. (2001). From attention to action in frontal cortex. In J. Braun & C. Koch (Eds.), *Visual attention and cortical circuits* (pp. 137–157). Cambridge, MA: MIT Press.

To, D., Lau, R. W. H., & Green, M. (2001). An adaptive multiresolution method for progressive model transmission. *Presence-Teleoperators & Virtual Environments, 10,* 62–74.

Treisman, A. M., & Gelade, G. (1980). A feature-integration theory of attention. *Cognitive Psychology, 12,* 97–136.

van Diepen, P. M. J., Ruelens, L., & d'Ydewalle, G. (1999). Brief foveal masking during scene perception. *Acta Psychologica, 101,* 91–103.

ViewGraphics Incorporated (Model 6000). Mountain View, CA: Author.

Wang, Z., & Bovik, A. C. (2001). Embedded foveation image coding. *IEEE Transactions on Image Processing, 10,* 1397–1410.

Williams, D. E., & Reingold, E. M. (2001). Preattentive guidance of eye movements during triple conjunction search tasks: The effects of feature discriminability and saccadic amplitude. *Psychonomic Bulletin & Review, 8,* 476–488.

Wolfe, J. M. (1994). Guided search 2.0: A revised model of visual search. *Psychonomic Bulletin & Review, 1,* 202–238.

Yang, J., Coia, T., & Miller, M. (2001). Subjective evaluation of retinal-dependent image degradations. *Proceedings of PICS 2001: Image Processing, Image Quality, Image Capture Systems Conference* (pp. 142–147). Springfield, VA: The Society for Imaging Science and Technology.

Received September 4, 2001
Revision received March 6, 2002
Accepted March 6, 2002 ■